Polymer 55 (2014) 2780–2791

Contents lists available at ScienceDirect

Polymer

journal homepage: www.elsevier.com/locate/polymer

Protein immobilization onto poly (vinylidene fluoride) microporous membranes activated by the atmospheric pressure low temperature plasma

Naohisa Akashi [a,*], Shin-ichi Kuroda [b]

[a] Graduate School of Engineering, Gunma University, 29-1 Hon-cho, Ohta, Gunma 373-0057, Japan
[b] Faculty of Science and Technology, Gunma University 29-1 Hon-cho, Ohta, Gunma 373-0057, Japan

ARTICLE INFO

Article history:
Received 13 January 2014
Received in revised form
29 March 2014
Accepted 15 April 2014
Available online 25 April 2014

Keywords:
Surface modification
Plasma
Poly (vinylidene fluoride)

ABSTRACT

Hydrophobic poly (vinylidene fluoride) (PVDF) membrane surface was treated with atmospheric pressure low temperature plasma and investigated physical and chemical surface characterization. The contact angle of water on the exposed membrane surface was reduced with increasing of the treatment voltage and time, so indicates that the treatments can modify the PVDF membrane surface from hydrophobic to hydrophilic. In order to analyze the phenomenon in detail, the progress of defluorination including dehydrofluorination and oxidation reactions onto the surface was examined by X-ray photoelectron spectroscopy (XPS), and revealed the most effective treatment condition. The degree of grafting used acrylic acid monomer onto the surface has influenced with monomer concentration, reaction temperature and reaction time. Scanning electron microscopy (SEM) and atomic force microscopy (AFM) were employed to study the surface morphology. The membrane surfaces conjugated bovine serum albumin (BSA) as a protein were surely detected the nitrogen element contained with BSA.

1. Introduction

Fluoropolymers have excellent features such as electrical and chemical resistance, high temperature stability and low surface energy [1,2]. Therefore, fluorinated polymers are applied in a variety of industries, for example medical equipment, engineering plastics, microelectronics, opto electronics, architectural fabrics and microwaveable coatings [3]. As some of the commercially available fluoropolymers, for example there are poly (tetrafluoroethylene) (PTFE) [4,5], poly(vinylidene fluoride) (PVDF) [6], Poly(tetrafluoroethylene-co-perfluoropropylvinylether) (PFA) [7,8] and Poly(tetrafluoroethylene-co-hexafluoropropylene) (FEP) [9,10]. In these, PVDF is especially one of the fluorocarbon polymers which can be used widely as a membrane material [11]. Hydrophobic PVDF membranes have a characteristic property which substantially interacts with proteins by hydrophobic interaction, so it is suitable for analysis applications which is identified or detected the small amount of target protein. On the other hand, hydrophilized PVDF membranes have been mainly adopting in the manufacturing processes for obtaining pharmaceutical drug substances or products for biologics from some decades ago. Filtration membranes are generally classified with microfiltration (MF), ultrafiltration (UF) and reverse osmosis (RO) according to pore size. In the manufacturing processes such as monoclonal antibodies (mAbs) and recombinant gene proteins for medical use, MF is almost applied for the prefiltration in order to raise filtration efficiency in UF, and remove bacteria, mycoplasma and cells. UF is often utilized for concentration of the target protein, buffer exchange and virus clearance which is required for biologically derived therapeutics in a process solution. From the above, membrane filtration is attractive because it is simple to operate and causes minimal damage, even for products that are highly labile to heat, radiation, or chemical treatment [12].

In recent years, many functionalized membranes by surface modifications have been reported [13–18]. As reported in the literature [19,20], there are ion-exchange MF membranes that anion exchange groups are cross-linked with regenerated cellulose membrane, and hydrophobic interaction MF membranes which introduced the phenyl groups, and human γ-globulin adsorption capacity of PVDF hollow fiber affinity membranes containing different amino acid ligands [21]. Therefore, unlike a conventional separation mechanism such as size exclusion, the membrane chromatography is one of the excellent technique of the flow through type that is

* Corresponding author.
E-mail address: akashi.n@jcom.home.ne.jp (N. Akashi).

http://dx.doi.org/10.1016/j.polymer.2014.04.029

designed for removing a relatively small amount of impurities such as deoxyribonucleic acid, endotoxin [22], host cell protein, and virus in a production process by peculiar interaction [23,24]. As different impurities, there are protein aggregates and cleaved products which is a common though undesirable occurrence or post-translational modification. Size exclusion chromatography which is used for preparative separation of mAb aggregates is slow and results in poorly resolved peaks, particularly for higher order aggregates. Lu Wang et al. have reported that a hydrophobic interaction membrane chromatography (HIMC) based method was rapidly and efficiently separation and analysis of mAb aggregates [25]. These surface modified membranes are generally offered as a single-use or disposable in order to reduce cleaning validation requirements in comparison with conventional ion-exchange or hydrophobic interaction chromatography resin.

As a method of surface modifications, there is the dry process that is clean and energy saving, and plasma processing [26–31], gamma irradiation [32,33], ultraviolet irradiation [34–38], photo-irradiation [39,40] are reported. In case of plasma processing with vacuum, there are some problems, for example, it is necessary to use a powerful pump and robust chamber in order to generate a vacuum condition, and it takes time before reaching a vacuum. On the contrary, in the atmospheric pressure low temperature plasma [41–45], it does not need equipment for vacuum processing, and partial surface treatment is possible. It is also applicable for the surface treatment of thermostable low materials because of low temperature processing. Plasma induced free radical polymerization is a useful technique for grafting acrylic polymers onto the surface of an inert polymeric substrate such as, Teflon, PVDF, PE, etc. [46].

In this study, we proposed the procedure for surface modification in order to immobilize target protein onto PVDF membranes initiated by atmospheric pressure low temperature plasma [47]. At first, we treated with hydrophobic PVDF membrane surface by argon plasma, and then exposed to air in order to modify highly reactive hydrophilic functional groups. Secondly, graft polymerization by acrylic acid monomer is performed onto the membrane surface in order to form carboxy groups. Thirdly, after the treatment for crosslinking is employed in order to prepare amine-reactive esters, bovine serum albumin (BSA) is finally conjugated onto the membrane surface. The surface properties are characterized by contact angle of water measurement, attenuated total reflection (ATR) Fourier transform infrared (FT-IR) spectroscopic analysis, scanning electron microscopy (SEM), X-ray photoelectron spectroscopy (XPS) and atomic force microscopy (AFM) [48].

2. Experimental

2.1. Materials

Hydrophobic membrane PVDF (Durapore®, 0.45 μm pore size) was purchased from Merck Millipore Corp. which was commercially named HVHP. N-Hydroxysulfosuccinimide (Sulfo-NHS), 1-(3-Dimethylaminopropyl)-3-ethylcarbodiimide HCl (EDC) and 2(N-morpholino)ethanesulfonic acid (MES) were purchased from ProteoChem, Inc. Acrylic acid (AAc) monomer and bovine serum albumin (BSA) were purchased from Sigma–Aldrich Co. LLC. AAc was distilled in nitrogen atmosphere prior to use. PBS (−) was purchased from Nissui Pharmaceutical Co., Ltd. The purity of argon gas was more than 99.99%. Distilled water was used in all experiments.

2.2. Plasma reactor and plasma treatments

Fig. 1 shows the equipment used in this study. It consists of a high frequency pulse power supply, a gas supply unit and the cold atmospheric pressure plasma torch (CAPPLAT) (Fig. 1(a)) [49,50]. The CAPPLAT has a cylindrical structure in which the plasma is generated. The plasma is blown out through the end of the CAPPLAT which consists of two co-axial cylindrical electrodes (Fig. 1(b)). The inner electrode, a copper tube (OD: 8 mm, ID: 7 mm), is connected to the power supply. The outer electrode (thickness: 1 mm, length: 20 mm) is made of aluminum and grounded. As a dielectric barrier, a silicone tube (thickness: 2.5 mm) is placed between the two electrode. The outlet of the CAPPLAT is embedded in the edge of a perforated silicone tube.

2.3. Chemical functionalization

Prior to the surface modification experiment, the PVDF membrane was rinsed with ethanol in an ultrasonic washer and dried at room temperature for 12 h. For plasma treatment of the PVDF membrane, argon gas was fed into the CAPPLAT at a flow rate of 5 L min^{-1} and the plasma was generated under the following conditions; applied voltage of ±4 kVp-p, frequency of 20 kHz, treatment time of 180 s and duty cycle of 50%. The PVDF membrane was treated with plasma at the position of 20 mm away from the torch end. Subsequently, the PVDF membrane was exposed to air for 20 min. The air-exposed membrane was immersed in an aqueous solution containing 20%(v/v) of AAc monomer. After bubbling with nitrogen for 20 min to remove dissolved oxygen, the ampoule was sealed and heated at 70 °C to initiate graft polymerization. The PVDF membrane grafted with polyacrylic acid (hereafter called PVDF-g-PAAc) was rinsed with distilled water to remove nongrafted monomers for 12 h. Graft yield was determined from initial and final weight obtained using a balance measuring to an accuracy of 0.05 mg.

The degree of grafting was calculated as the weight increase of the membrane according to the following equation [51,52]:

$$\text{Degree of Grafting (G\%)} = \frac{Wg - Wo}{Wo} \times 100$$

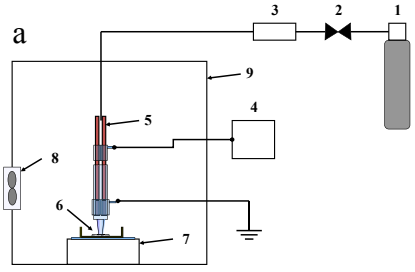

(1) argon gas cylinder; (2) valve; (3) mass flow meter; (4) power supply; (5) torch; (6) substrate; (7) stage; (8) exhaust fan; (9) reaction chamber

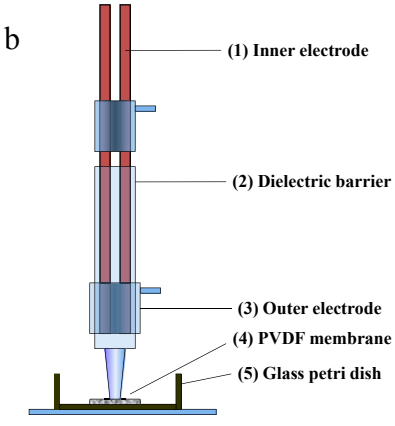

Fig. 1. Schematic structure of (a) plasma reactor and (b) CAPPLAT.

where Wg is the weight of the grafted membrane and Wo is the weight of the membrane.

BSA was grafted on PVDF-g-PAAc membrane surface using the EDC/NHS method. The PVDF-g-PAAc membrane was activated with 4 mmol l^{-1} EDC, 10 mmol l^{-1} Sulfo-NHS in 100 mmol l^{-1} MES, 500 mmol l^{-1} NaCl pH 6.0 buffer for 15 min at room temperature. The conjugation of BSA was carried out in a solution of 1 mg ml^{-1} BSA in 100 mmol l^{-1} MES, 500 mmol l^{-1} NaCl pH 6.0 buffer under mild agitation for 3 h at room temperature. The membrane (hereafter called PVDF-g-PAAc-BSA) was rinsed with a solution of PBS (−) to remove loosely absorbed BSA and MES buffer for 12 h.

2.4. Physical and chemical surface characterization

KYOWA KAIMEN KAGAKU CA-D was used to measure static contact angle of water of the membranes using a sessile drop method. The angles reported were reliable to ±1°. For each angle reported, at least five sample readings from different surface locations were averaged.

To study the surface chemical composition changes of the membranes, attenuated total reflection (ATR) Fourier transform infrared (FT-IR) spectroscopic investigations were carried out with a Nicolet MAGNA IR560 spectrometer using a Ge crystal. The spectra were measured in the wave number range of 1000 − 4000 cm^{-1}. The spectra were collected by cumulating 64 scans at a resolution of 4 cm^{-1}. All ATR–FTIR spectra were recorded at ambient temperature.

X-ray photoelectron spectroscopy (XPS) was used to analyze the chemical composition of the untreated and functionalized PVDF membranes and was performed on a Kratos AXIS Nova spectrometer using a monochromatized Al Kα X-ray source (1486.6 eV photons). The base pressure in the analytical chamber was maintained at 10^{-8} Torr or lower during each measurement. All measurements were made at a photoelectron takeoff angle of 45°. The Kratos charge neutralizer system was used on all specimens. The X-ray source was run at a reduced power of 150 W (15 kV and 10 mA). The samples were mounted on the standard sample plate by means of adhesive tapes. Survey scan analyses were carried out at a constant dwell time of 100 ms, pass energy of 160 eV and energy resolution of 1 eV. High resolution analyses were carried out at a constant dwell time of 200 ms, pass energy of 20 eV and energy resolution of 0.1 eV. All binding energies (BEs) were referenced to the C1s hydrocarbon peak at 286.4 eV. Spectra were analyzed using XPSPEAK software (version 4.1). Curve fitting of the high resolution spectra used 30% Gaussian/70% Lorentzian mixed line shapes for each component.

2.5. Membrane morphology

The surface and cross-section morphologies of the membranes were examined by scanning electron microscopy (SEM), using a Hitachi S-3000N electron microscope. The samples were mounted on the standard sample plate by means of adhesive tapes. A thin layer of Pt was sputtered on the sample surface prior to the SEM measurement. For cross-sectional view studies, the membrane was fractured under liquid nitrogen. A thin layer of platinum was sputtered onto the cross-sectional surface prior to the SEM measurement. The SEM measurements were performed at an accelerating voltage of 15.0 kV.

An atomic force microscopy (AFM, Seiko Instruments SPA-400) was also used to further study the surface topography change of the membrane. AFM images were acquired in the dynamic force mode with a cantilever (SI-DF20, Seiko Instruments). To investigate surface roughness of each sample, it was calculated average roughness (*Ra*). From the direction of the average line of the roughness curve of a sampled standard length (L), plot the direction of the average line of the sampled section on the *X* axis and the direction of the vertical magnification on the *Y* axis, and express the roughness curve using the equation $y = F(x)$. The roughness value was then expressed in nanometers as the value determined from the following expression.

$$\mathrm{Ra\ (nm)} = \frac{1}{L}\int_0^L |F(x)|\mathrm{d}x$$

3. Results and discussion

Scheme 1 shows a schematic diagram illustrating the process of surface modifications. As a first step, the surface of PVDF membrane was treated with argon plasma. The plasma-treated samples are

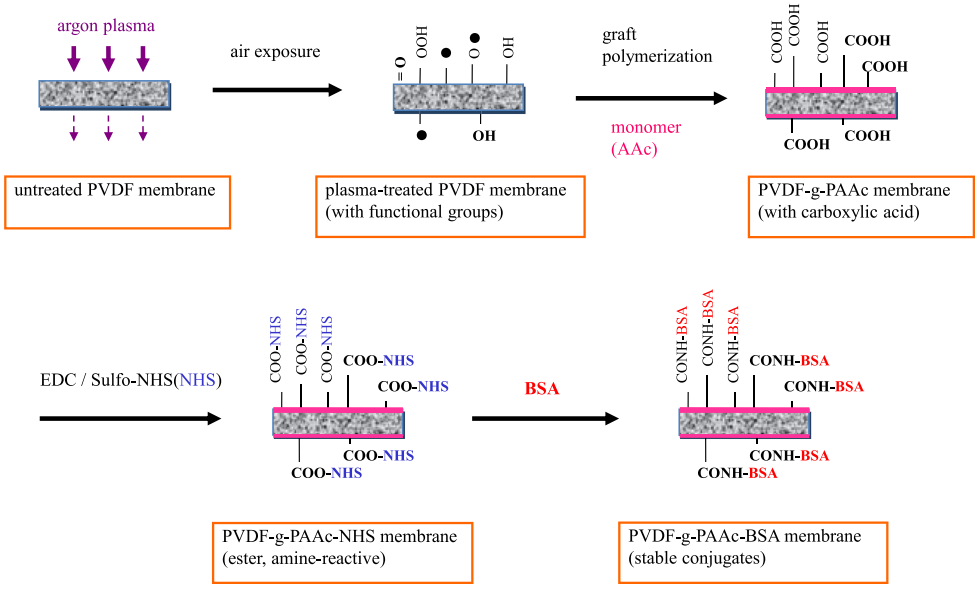

Scheme 1. Schematic illustration of the surface modifications by graft polymerization of AAc.

generally exposed to air in order to generate peroxide and hydroperoxide initiator species. AAc was graft polymerized in the solution by thermal initiation. After EDC/Sulfo-NHS reaction step, BSA was conjugated on the carboxy groups of the PVDF-g-PAAc membrane surface. Subsequently, PVDF-g-PAAc-BSA membrane was fabricated for immobilizing onto the aminated surface of the PVDF-g-PAAc-NHS membrane.

3.1. Hydrophilicity characterization

Plasma contains activated species which are able to initiate chemical and physical reactions on the solid surfaces of polymers. When polymers are exposed to plasma, essentially degradation reactions such as polymer chain scission and cross-linking initiate. On the other hand, functional groups for example hydroperoxide and carboxy groups will be formed on the polymer surface. Fig. 2 shows the results of contact angle of water on the PVDF membrane surface, treated by argon plasma, as a function of plasma exposure time from 30 to 300 s and a voltage of ±2.8–5.0 kVp-p.

Beforehand, we confirmed that the contact angle on plasma-treated PVDF membrane before and after ethanol rinsing had less difference. The contact angle of the non-treated PVDF membrane was about value 119°. The contact angle on the exposed samples was reduced with increasing voltage. It was indicated that the plasma treatment could modify the PVDF membrane surface from hydrophobic to hydrophilic.

The contact angle of PVDF membrane treated with less than ±3.5 kVp-p for the same exposure time, decreased slowly reaching a similar value, and the appearance did not change from untreated samples. On the other hand, the contact angle of samples treated with ±4.0 kVp-p decreased almost linearly in the course of processing time, and the surface of the sample treated directly for more than 240 s exhibited a slightly burnt area, which means it contained a little amount of degradation products. In case of samples modified with more than ±4.5 kVp-p, the contact angle decreased rapidly up to 60 s. Beyond 60 s the contact angle decreased gradually. However, the appearance of the samples was intensively burnt after 60 s. From these results, we realized that plasma treatment of more than ±4.5 kVp-p led heavy etching reaction, and plasma treatment during 30–180 s and ±2.8–4.0 kVp-p could prevent the etching reaction. Hence, we recognized that the treatment time of 180 s and the voltage of ±4.0 kVp-p were the most effective condition for mild surface modification.

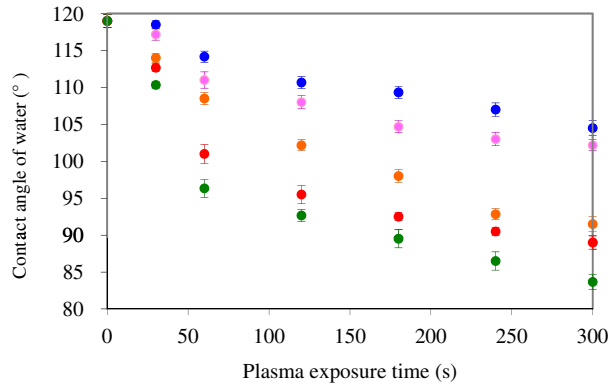

Fig. 2. Contact angle of water on PVDF membrane surface treated with argon plasma as a function of plasma exposure time and voltage: (blue) ±2.8 kVp-p, (pink) ±3.5 kVp-p, (orange) ±4.0 kVp-p, (red) ±4.5 kVp-p, (green) ±5.0 kVp-p. Data are presented as means ± SD. (For interpretation of the references to color in this figure legend, the reader is referred to the web version of this article.)

3.2. Dependence of the degree of grafting on reaction conditions

PAAc was grafted onto the plasma-treated PVDF membrane surface by thermal polymerization method. The grafting yield for a typical plasma-induced free radical polymerization depends on some factors, such as plasma treatment time, plasma power, monomer concentration, reaction temperature, reaction time. In this work, the attention has been focused on the following factors: monomer concentration, reaction temperature and reaction time.

First of all, Fig. 3(a) shows the effect of monomer concentration from 10 to 30%(v/v) on the grafting yield of PAAc. The grafting yield increased with increasing the monomer concentration, especially more than 20%(v/v). Secondly, Fig. 3(b) indicates the effect of polymerization reaction temperature from 50 to 90 °C. The grafting yields increased gradually depending on increasing the reaction

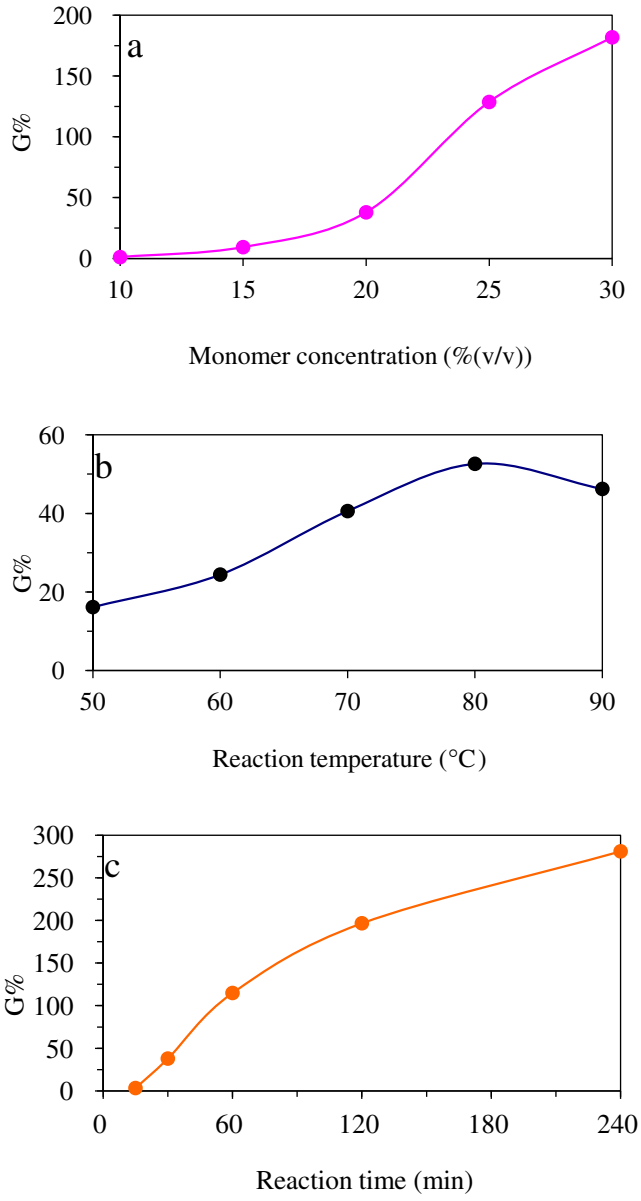

Fig. 3. The effect of (a) monomer concentration (treatment: 30 min, 70 °C), (b) reaction temperature (treatment: 20%(v/v) AAc, 30 min) and (c) reaction time (treatment: 20%(v/v) AAc, 70 °C) on the grafting yield of PAAc. Data are presented as means from 3 independent substrates.

temperature up to 80 °C, and then decreased after passing through a maximum. Thirdly, Fig. 3(c) represents the effect of polymerization reaction time. The grafting yield increased with increasing the reaction time. It was found that the graft yield of sample treated with monomer 20%(v/v) for 60 min (Fig. 3(c)) was approximately the same value as that of the treated with 25%(v/v) for 30 min (Fig. 3(a)). Furthermore, we realized that monomer concentration and treatment time should be controlled especially as graft conditions.

If the amount of PAAc chains on the membrane surface, including the pore surface is larger, the yield of protein immobilization will decrease because of the limited surface area. Considering the scale-up of this polymerization process, it was thought that lower monomer concentration, treatment time and temperature would be preferable in terms of cost effectiveness. Therefore, we decided that the monomer concentration of 20%(v/v), reaction time of 30 min and temperature of 70 °C were the optimum conditions for the graft polymerization.

3.3. Structure characterization of the membranes by ATR–FTIR analysis

Fig. 4 shows the respective ATR–FTIR spectra of (a) untreated PVDF membrane, (b) PVDF membrane treated with argon plasma, PVDF-g-PAAc membranes grafted with AAc for (c) 15 min, (d) 30 min, and PVDF-g-PAAc-BSA membranes covalently immobilized with the BSA concentration of (e) 0.08 mg ml^{-1}, (f) 1.00 mg ml^{-1}.

For comparison purpose, the ATR–FTIR spectrum of the untreated PVDF membrane is shown in Fig. 4. The absorption bands at 1070–1236 cm^{-1} are characteristic bands of CF_2 functional group of PVDF (Fig. 4(a)). The ATR–FTIR spectrum of the PVDF membrane treated with argon plasma contained a weak absorption band at 1707 cm^{-1} which was associated with C=O stretching of the carbonyl group (Fig. 4(b)).

The ATR–FTIR spectrum of the PVDF-g-PAAc membrane grafted with AAc for 30 min (Fig. 4(d)) appeared with stronger, C=O absorption stretching band that compared with the sample grafted for 15 min (Fig. 4(c)). It was proved that the grafting yield increased depending on the reaction time. The ATR–FTIR spectrum of the PVDF-g-PAAc membrane grafted with AAc for 30 min was also exhibited a broad OH stretching absorption band between 3300 and 2500 cm^{-1}. It was suggested that polyacrylic acid chains were successfully grafted onto the surface of the PVDF membrane qualitatively. The acid function of the PVDF-g-PAAc membrane must be activated by EDC to react with the BSA amino group.

The ATR–FTIR spectra of the PVDF-g-PAAc-BSA membrane shows a characteristic –NH stretching absorption band. Especially, the ATR–FTIR spectrum of the PVDF-g-PAAc-BSA membrane covalently functionalized with the BSA concentration of 1.00 mg ml^{-1} (Fig. 4(f)) was found having a stronger –NH stretching absorption band at 1554 cm^{-1} that compared with the sample immobilized with the BSA concentration of 0.08 mg ml^{-1} (Fig. 4(e)). It was suggested that the immobilizing yield increased with the BSA concentration and BSA were suitably conjugated onto the surface of the PVDF-g-PAAc membrane largely. Furthermore, broad absorption bands attributed to primary amino groups with maximum at 3400 cm^{-1} were observed (Fig. 4(f)). On the other

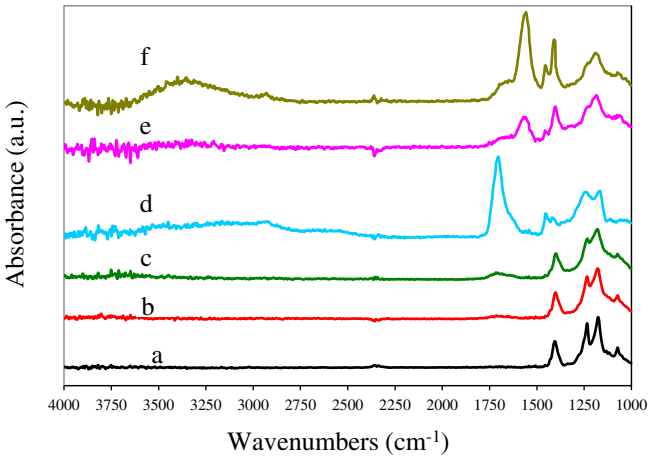

Fig. 4. ATR–FTIR spectra of (a) untreated PVDF membrane, (b) PVDF membrane treated with argon plasma (treatment: ±4.0 kVp-p, 180 s), PVDF-g-PAAc membranes grafted with AAc for (c) 15 min, (d) 30 min (treatment: 20%(v/v) AAc, 70 °C), and PVDF-g-PAAc-BSA membranes covalently immobilized with the BSA concentration of (e) 0.04 mg ml^{-1}, (f) 1.00 mg ml^{-1} (treatment: 3.0 h).

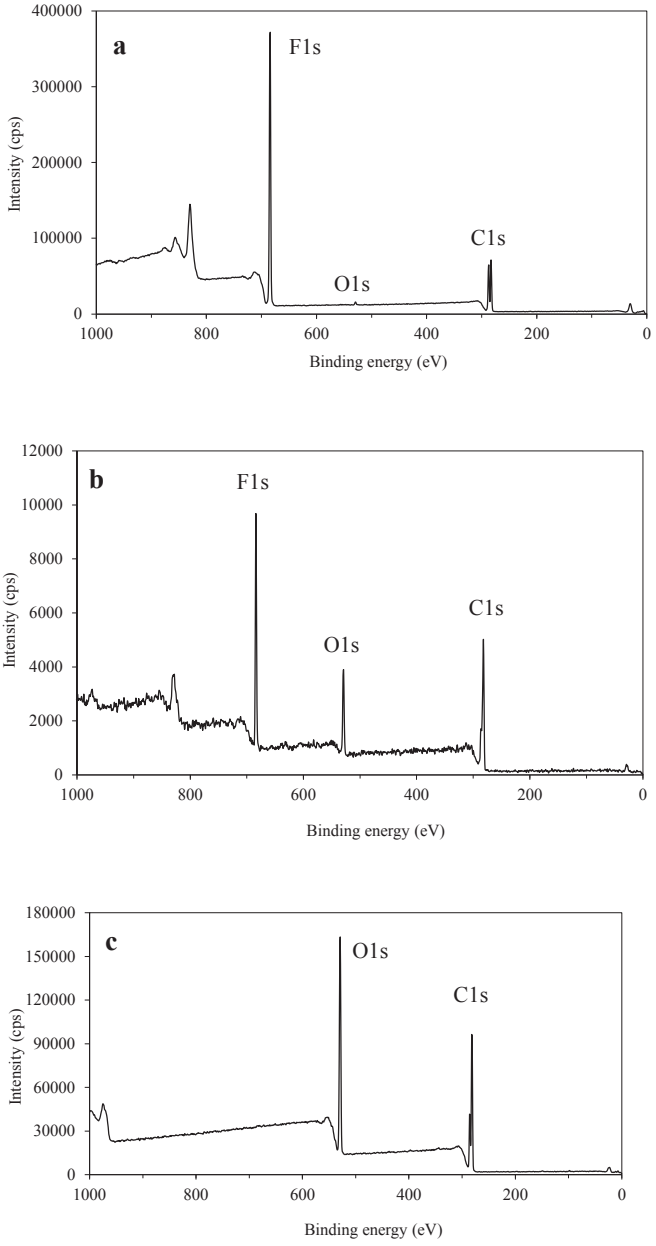

Fig. 5. XPS survey scan of (a) untreated PVDF membrane, (b) PVDF membrane treated with argon plasma (treatment: ±4.0 kVp-p, 180 s) and (c) PVDF-g-PAAc membranes (treatment: 20%(v/v) AAc, 70 °C, 30 min).

Table 1
Atomic ratios of PVDF membrane surface exposed to argon plasma.

Plasma treatment			Atomic ratio		Defluorination (%)
Voltage (±kVp-p)	Flow rate (L min^{-1})	Exposure time (s)	F/C	O/C	
–	–	–	1.01	0.01	0
4.0	5	60	0.50	0.16	50
4.0	5	180	0.38	0.20	62
4.0	5	300	0.31	0.20	69
2.8	5	180	0.58	0.14	43
4.0	5	180	0.38	0.20	62
5.0	5	180	0.32	0.21	68
4.0	4	180	0.42	0.19	58
4.0	5	180	0.38	0.20	62
4.0	6	180	0.43	0.18	57

hand, the bands corresponding to the carboxylic acids and CF_2 functional group indicated a weak absorption.

3.4. Structure characterization of the membranes by XPS analysis

The XPS survey spectra of (a) untreated PVDF membrane, (b) PVDF membrane treated with argon plasma and (c) PVDF-g-PAAc membranes are shown Fig. 5.

Two peaks at BEs of 286 and 291 eV attributable to C1s and a strong peak at BE of 688 eV attributable to F1s were observed in the XPS survey scan spectrum of the non-treated hydrophobic PVDF membrane (Fig. 5(a)). The XPS survey scan spectrum of the PVDF membrane treated with argon plasma consisted of peaks at BEs of 286, 291, 534, and 688 eV, attributable to C1s, C1s, O1s, and F1s, respectively (Fig. 5(b)). On the other hand, the result of the XPS measurement onto PVDF-g-PAAc membrane consisted of peaks at BEs of 285, 289, and 533 eV, attributable to C1s, C1s, and O1s, respectively (Fig. 5(c)). It shows that successful grafting of PAAc on the plasma-treated membrane was performed since the fluorine content on the surface decreased substantially after grafting.

Atomic composition for the PVDF membrane surfaces modified by argon plasma was estimated from relative intensities of C1s, F1s, and O1s high resolution spectra. Results of XPS analysis for the F/C and O/C atom ratios of the PVDF membrane surface treated with argon plasma are summarized in Table 1.

The weak peak at BEs of 533 eV on the survey spectrum of untreated PVDF, attributable to O1s signal, confirmed that the PVDF surface was partially oxidized. However, the O/C atom ratio for the untreated PVDF was 0.01, so it was considered to be low level. All plasma-treated PVDF membrane surfaces showed lower F/C atom ratio than the untreated PVDF surface, and higher O/C atom ratio. In other words, a reduction in fluorine intensity occurred together with an increase in oxygen intensity and relative increase in the

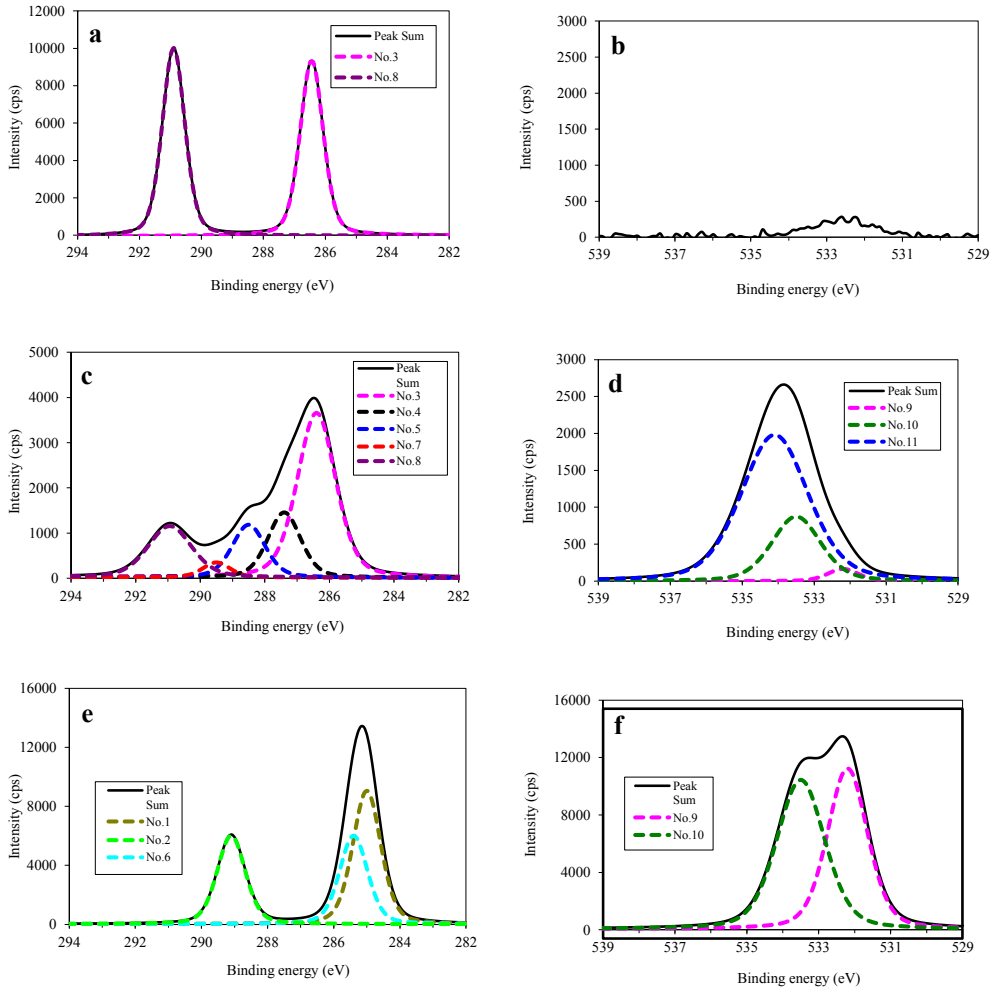

Fig. 6. High resolution XPS spectra of C1s (a, c, e) and O1s (b, d, f): (a, b) untreated PVDF membrane, (c, d) PVDF membrane treated with argon plasma (treatment: ±4.0 kVp-p, 180 s) and (e, f) PVDF-g-PAAc membrane (treatment: 20%(v/v) AAc, 70 °C, 30 min). The peak numbers in these figures corresponds to the Peak No. of Table 2.

carbon. These changes indicate that the plasma exposure led to defluorination including dehydrofluorination and oxidation reactions on the PVDF membrane surfaces.

In this work, we investigated the influence of defluorination and oxidation on the plasma treatment time, applied voltage and flow rate of argon gas. Firstly, defluorination estimated from the F/C atom ratio increased by 50% in 60 s, 62% in 180 s, and 69% in 300 s at ±4.0 kVp-p compared to untreated PVDF. Secondly, defluorination resulted in 43% at ±2.8 kVp-p, 62% at ±4.0 kVp-p, and 68% at ±5.0 kVp-p in 180 s compared to untreated PVDF. Therefore, with increasing the treatment time and voltage, defluorination was gradually in progress. It was also confirmed that defluorination was occurred even at the minimum voltage of ±2.8 kVp-p when plasma could be formed. Likewise, oxidation reaction estimated from the O/C atom ratio was also progressed by increasing the rate of the plasma treatment time and applied voltage, however oxidation was approximately the same beyond 180 s or ±4.0 kVp-p. Finally, as a consequent of evaluating the effect of flow rate of argon gas on defluorination and oxidation, defluorination was 58% at 4 L min^{-1}, 62% at 5 L min^{-1}, and 57% at 6 L min^{-1} for 180 s compared to untreated PVDF. Similarly, oxidation was the most progressed in 20% at 5 L min^{-1}, whereas it was almost at the same level between 4 L min^{-1} and 6 L min^{-1}. Collectively, it was concluded that the most effective flow rate of argon gas was 5 L min^{-1} to abstract fluorine atoms from untreated PVDF and produce reactive sites on the membrane surface for further modification.

To discuss defluorination, dehydrofluorination and oxidation reactions in detail, we investigated the data of narrow scanning C1s and O1s core level spectra. Fig. 6 shows C1s and O1s spectra for untreated PVDF membrane, PVDF membrane treated with argon plasma and PVDF-g-PAAc membrane. The decomposed peaks were illustrated in dotted lines.

Table 2 summarizes the BEs and functional groups from the results of high resolution XPS analysis.

The C1s high resolution spectrum of untreated PVDF membrane surface assigned to two distinct peaks at BEs of 286.4 eV (due to CF_2–$\underline{C}H_2$–CF_2:No.3) and 290.9 eV (due to CH_2–$\underline{C}F_2$–CH_2:No.8). Plasma-treated PVDF membrane and PVDF-g-PAAc membrane showed complex C1s spectra. The underlined C or O in these linkages means the objective carbon or oxygen, and each number of decomposed peaks corresponds with peak number in Table 2.

The C1s high resolution spectrum of plasma-treated PVDF membrane was decomposed into five peaks as shown in Table 2. The five peaks appeared at BEs of 286.4, 287.4, 288.5, 289.5 and 290.9 eV, which were assigned to CF_2–$\underline{C}H_2$–CF_2, CH_2–$\underline{C}F$=CH, CH_2–$\underline{C}F$=CH_2 and hydroperoxide (CH_2–$\underline{C}H$(–OOH)–CH_2) groups (No.3); hydroperoxide (CF_2–$\underline{C}H$(–OOH)–CF_2) (No.4); carbonyl (CF_2–$\underline{C}HO$) and CH_2–$\underline{C}FH$–CH_2 groups (No.5); hydroperoxide (CH_2–$\underline{C}F$(–OOH)–CH_2) (No.7); and CH_2–$\underline{C}F_2$–CH_2 and carbonyl (CH_2–$\underline{C}FO$) and CH=$\underline{C}F_2$ groups (No.8), respectively. The composition in Fig. 6(c) indicates surely that CF_2 carbons were modified into $\underline{C}FH$, $\underline{C}$(–OOH) and $\underline{C}FO$ carbons in the plasma exposure. On the other hand, the C1s high resolution spectrum of PVDF-g-PAAc membrane was decomposed into characteristic three peaks attributable to AAc graft polymerization. The three peaks observed at BEs 285.0, 285.4, and 289.1 eV, which were individually assigned to –CH(COOH)–$\underline{C}H_2$–CH(COOH)– (No.1); $\underline{C}H$–COOH (No.2); and carboxy (CH–$\underline{C}OOH$) group (No.6).

Likewise, the O1s high resolution spectrum of plasma-treated PVDF membrane was curve-fitted with three peaks at BEs of 532.2 eV for carbonyl (CH_2–$CF\underline{O}$) and aldehyde (CF_2–$CH\underline{O}$) groups (No.9), 533.5 eV for hydroperoxide (CH_2–CF(–$\underline{O}$OH)–CH_2, CF_2–CH(–$\underline{O}$OH)–CF_2) groups (No.10) and 534.0 eV for hydroperoxide (C–O$\underline{O}$H:No.11). On the other hand, the O1s high resolution

Table 2
Summary of high resolution XPS scan results for untreated PVDF membrane, PVDF membrane treated with argon plasma (treatment: ±4.0 kVp-p, 180 s) and PVDF-g-PAAc membrane (treatment: 20%(v/v) AAc, 70 °C, 30 min). When it is considered that some functional groups are included in each peak, these groups are identified by a number. Values represent the percentage associated to each or sum of bond type. Note that (–) denotes 0%. The underlined C or O means the objective carbon or oxygen.

Peak no.	BEs (eV)	Functional groups	Untreated PVDF	Plasma-treated PVDF	PVDF-g-PAAc
1	285.0	–CH(COOH)–$\underline{C}H_2$–CH(COOH)–	–	–	43.0
2	285.4	>$\underline{C}$H-COOH	–	–	28.5
3	286.4	(1) –CF_2–$\underline{C}H_2$–CF_2– (2) –CH_2–$\underline{C}F$=CH– (3) –CH_2–$\underline{C}F$=CH_2 (4) –CH_2–$\underline{C}H$(–OOH)–CH_2–	(1) 48.7	(1,2,3,4) 49.2	–
4	287.4	–CF_2–$\underline{C}H$(–OOH)–CF_2–	–	16.7	–
5	288.5	(1) –CF_2–$\underline{C}HO$ (2) –CH_2–$\underline{C}FH$–CH_2–	–	(1,2) 13.5	–
6	289.1	>CH-$\underline{C}$OOH	–	–	28.5
7	289.5	–CH_2–$\underline{C}F$(–OOH)–CH_2–	–	3.2	–
8	290.9	(1) –CH_2–$\underline{C}F_2$–CH_2–(2) –CH_2–$\underline{C}FO$ (3) –CH=$\underline{C}F_2$	(1) 51.3	(1,2,3) 17.5	–
9	532.2	>CH-C$\underline{O}$OH (2) –CH_2–CF$\underline{O}$ (3) –CF_2–CH$\underline{O}$	–	(2,3) 2.8	(1) 47.4
10	533.5	>CH-CO$\underline{O}$H (2) –CH_2–CF(–$\underline{O}$OH)–CH_2– (3) –CF_2–CH(–$\underline{O}$OH)–CF_2–	–	(2,3) 23.6	(1) 52.6
11	534.0	≥C-O$\underline{O}$H	–	73.6	–

spectrum of PVDF-g-PAAc membrane was integrated with typical two peaks at BEs of 532.2 eV for carboxy group (CH–COOH:No.9) and 533.5 eV for carboxy group (CH–COOH : No.10).

3.5. The activation mechanism for initiation of graft polymerization

We attempted to elucidate the activation mechanism for PVDF membrane surface occurred by argon plasma treatment. Since the metastable argon, which is the most important active species in the present plasma, has an energy level of 11.5 eV [53], the energy transfer from metastable argon to the collided atom results in the link cleavage. The effect is comparable to the vacuum UV irradiation [54]. The following reactions for (i) dehydrofluorination, (ii) defluorination and (iii) dehydrogenation were inferred from the results of high resolution XPS scan shown in Table 2. The combination number after every equation corresponds to the numbers of peak and functional groups shown in Table 2, which means the resultant structure. For example, (3-2) shows the functional group (2) in peak No.3, and (7) is consistent with the functional group of peak No.7.

(i) A possible reaction of dehydrofluorination originated from plasma treatment is shown below.

$$-CH_2-CF_2-CH_2-CF_2- \rightarrow -CH_2-CF=CH-CF_2- + HF \qquad (3\text{-}2)$$

(ii) A possible reaction of defluorination occurred by plasma treatment is shown below.

$$-CH_2-CF_2-CH_2-CF_2- \rightarrow -CH_2-\dot{C}F-CH_2-CF_2- + {}^{\cdot}F$$

As a subsequent reaction, the distinct pathways would be considered.

1) The resulting radical leads to β-scission to yield the chain $-CF{=}CH_2$ double bond. However, it is assumed to the underlined carbon atom of $-CF{=}\underline{C}H_2$ is negligible owing to the result of Table 2.

$$-CH_2-\dot{C}F-CH_2-CF_2- \rightarrow -CH_2-CF=CH_2 + {}^{\cdot}CF_2- \qquad (3\text{-}3)$$

2) The resulting radical abstracts hydrogen from another polymer molecule.

$$-CH_2-\dot{C}F-CH_2-CF_2- \rightarrow -CH_2-CFH-CH_2-CF_2- \qquad (5\text{-}2)$$

Following the reaction of 2), it is also possible that the remaining fluorine atom bound to the defluorinated carbon atom is eliminated with successive plasma treatment.

Table 3
Summary of atomic composition about untreated PVDF membrane, PVDF membrane treated with argon plasma (treatment: ±4.0 kVp-p, 180 s), PVDF-g-PAAc membrane (treatment: 20%(v/v) AAc, 70 °C, 30 min) and PVDF-g-PAAc-BSA membrane (treatment: 1.00 mg ml^{-1} BSA, 3.0 h) measured by XPS. Note that (–) denotes 0.

Membranes	Atomic composition (%)				Atomic ratio	
	F	C	O	N	F/C	O/C
Untreated PVDF	50.0	49.7	0.3	–	1.01	0.01
Argon plasma-treated PVDF	23.8	62.9	12.5	0.8	0.38	0.20
PVDF-g-PAAc	–	65.8	34.0	0.1	–	0.52
PVDF-g-PAAc-BSA	5.3	64.1	27.1	3.6	0.08	0.42

$$-CH_2-CFH-CH_2-CF_2- \rightarrow -CH_2-\dot{C}H-CH_2-CF_2- + {}^{\cdot}F$$

The resulting radical formed hydroperoxide group through oxidation.

$$-CH_2-\dot{C}H-CH_2-CF_2- \xrightarrow{O_2} -CH_2-\underset{\displaystyle O-OH}{CH}-CH_2-CF_2- \qquad (3\text{-}4)$$

3) The resulting radical formed hydroperoxide group through oxidation.

$$-CH_2-\dot{C}F-CH_2-CF_2- \xrightarrow{O_2} -CH_2-\underset{\displaystyle O-OH}{CF}-CH_2-CF_2- \qquad (7)$$

If the cleavage of single bond in hydroperoxide group progresses, it occurs oxyl radical and hydroxyl radical as shown.

$$-CH_2-\underset{\displaystyle O-OH}{CF}-CH_2-CF_2- \rightarrow -CH_2-\underset{\displaystyle O^{\cdot}}{CF}-CH_2-CF_2- + {}^{\cdot}OH$$

Afterwards, the oxyl radical would suffer β-scission immediately to yield the chain –CFO.

$$-CH_2-\underset{\displaystyle O^{\cdot}}{CF}-CH_2-CF_2- \rightarrow -CH_2-\underset{\displaystyle O}{\overset{\displaystyle \|}{C}}F + {}^{\cdot}CH_2-CF_2- \qquad (8\text{-}2)$$

(iii) A possible mechanism of dehydrogenation originated from plasma treatment is shown below.

$$-CH_2-CF_2-CH_2-CF_2- \xrightarrow{\cdot R} -\dot{C}H-CF_2-CH_2-CF_2- + RH$$

1) The resulting radical leads to β-scission to yield the chain $-CH{=}CF_2$ double bond.

$$-\dot{C}H-CF_2-CH_2-CF_2- \rightarrow -CH=CF_2 + {}^{\cdot}CH_2-CF_2- \qquad (8\text{-}3)$$

2) The resulting radical formed hydroperoxide group through oxidation.

$$-CH_2-CF_2-\dot{C}H-CF_2- \xrightarrow{O_2} -CH_2-CF_2-\underset{\displaystyle O-OH}{CH}-CF_2- \qquad (4)$$

Likewise, if the cleavage of single bond in hydroperoxide group progresses, it occurs oxyl radical and hydroxyl radical as shown.

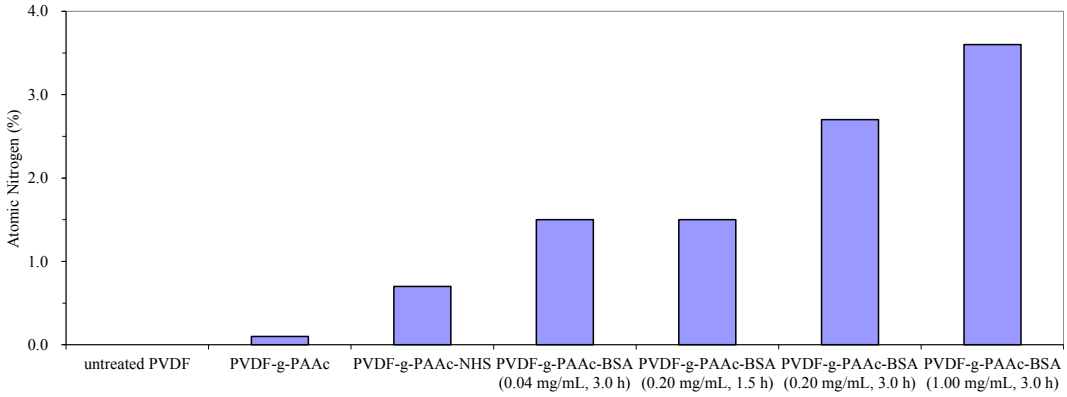

Fig. 7. XPS analysis of N1s levels for untreated PVDF membrane, PVDF-g-PAAc membrane (treatment: 20%(v/v) AAc, 70 °C, 30 min), PVDF-g-PAAc membrane provided a semi-stable Sulfo-NHS ester (PVDF-g-PAAc-NHS), and conjugated PVDF-g-PAAc-BSA (treatment: 1.00 mg ml^{-1} BSA, 3.0 h). Nitrogen levels are elevated in PVDF-g-PAAc-NHS due to the nitrogen in NHS. Conjugated BSA (as measured in terms of N content) increased with increasing BSA concentration in the conjugation solution and treatment time in case of 0.20 mg ml^{-1}.

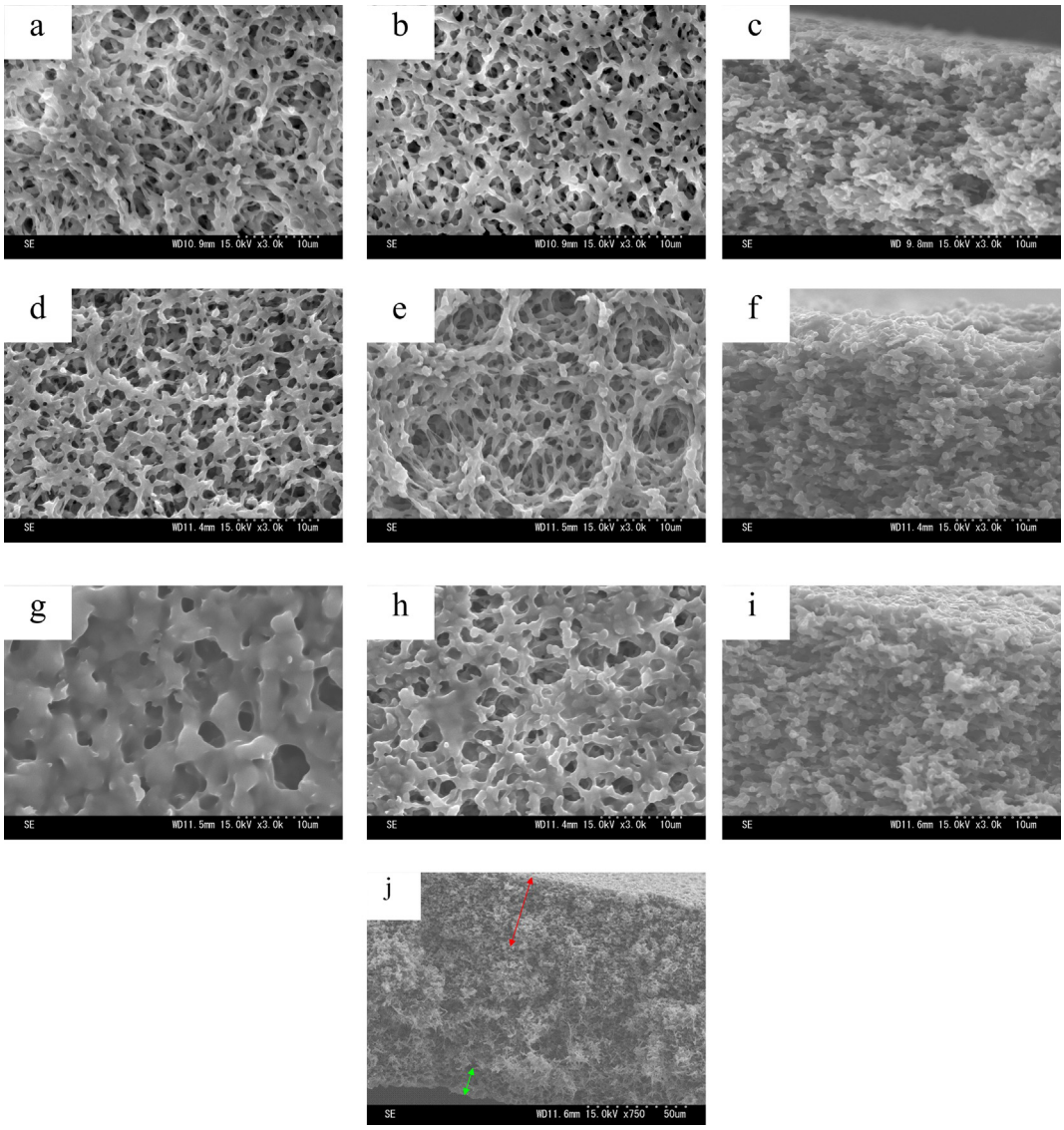

Fig. 8. SEM micrographs of untreated PVDF membrane (a, b, c), PVDF membrane treated with argon plasma (d, e, f; treatment: ±4.0 kVp-p, 180 s), and PVDF-g-PAAc membrane (g, h, i, j; treatment: 20%(v/v) AAc, 70 °C, 30 min). a, d, g: upper surface; b, e, h: bottom surface and c, f, i, j: cross section. These membranes were treated with argon plasma from the above of upper surface.

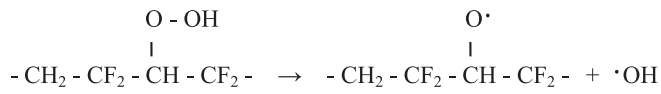

Afterwards, the oxyl radical would suffer β-scission immediately to yield the chain −CHO.

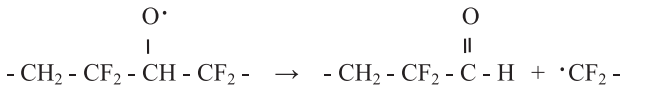

(5-1)

Table 2 shows that several hydroperoxide groups were produced on PVDF membrane treated with argon plasma. Therefore, we propose that hydroperoxide groups distributed on PVDF membrane treated with argon plasma were cleaved by thermal treatment, and originated some radicals induced to initiate graft polymerization.

3.6. Dependence of the degree of BSA conjugation on reaction conditions

Table 3 summarizes the atomic composition and the ratio of untreated PVDF, PVDF treated with argon plasma, PVDF-g-PAAc and PVDF-g-PAAc-BSA membranes. Nitrogen was also a target element monitored for two reasons. Firstly, PVDF is not constituted with nitrogen of the polymer elemental composition. Secondly, BSA is an approximately Mw 66 kDa protein contained nitrogen derived from its polypeptide backbone.

It can be seen that a small amount of nitrogen moieties is incorporated after plasma treatment and subsequent exposure to air. After grafting AAc onto plasma-treated PVDF membrane, atomic nitrogen percentage decreased as low as 0.1%. After covalently immobilizing BSA onto PVDF-g-PAAc membranes, atomic nitrogen percentage increased as high as 3.6%. However, fluorine was detected again onto PVDF-g-PAAc-BSA membrane. As a source of the phenomenon, it was assumed that the PAAc-ungrafted sites on PVDF-g-PAAc-BSA membrane surface were revealed, because the conformation of PAAc grafted onto PVDF-g-PAAc membrane had been changed due to the conjugation with BSA.

Fig. 7 shows that changes in the nitrogen content of untreated PVDF membrane, PVDF-g-PAAc membrane, PVDF-g-PAAc membrane provided a semi-stable Sulfo-NHS ester (PVDF-g-PAAc-NHS) and PVDF-g-PAAc-BSA membranes fabricated using a different BSA solution of 0.04, 0.20 and 1.00 mg ml^{-1}.

Activated PVDF-g-PAAc-NHS membrane showed 0.7% of nitrogen level, which is derived from the Sulfo-NHS. In order to investigate the effect of BSA concentration in the conjugation solution on the amount of nitrogen present, three different BSA concentrations were tested for 3.0 h as a fixed conjugation time. As shown in the Fig. 7, the nitrogen content increased significantly, suggesting that the conjugation reaction was concentration dependent. Likewise, in order to examine the relation between conjugation time and degree of BSA conjugation, we also conducted conjugation reactions for 1.5 h and 3.0 h using 0.20 mg ml^{-1} BSA solution. As can be seen, the nitrogen content increased successfully from 1.5% to 2.7%. Another finding is that the nitrogen content was the same for both BSA conjugation treatments at 0.04 mg ml^{-1} for 3.0 h and at 0.20 mg ml^{-1} for 1.5 h. Taken together, these results demonstrate that alterations of protein concentration and treatment time potentially contribute to protein immobilization.

3.7. Membrane morphology

The 3-D scaffolds of membranes in this work are intended for biotechnology application in order to maintain the area capable of interacting with the objective, so it is important that plasma treatment and subsequent AAc grafting reactions minimize the interference with their porosity. Thus, SEM images at magnification of 3000× for these membranes were taken before and after various chemical treatments in order to verify the impact on the porous structures and shown in Fig. 8. These membranes were treated with plasma from the above the upper surface.

In the features on the upper surface, the porous membrane fibers of the scaffolds for argon plasma treatment as shown in Fig. 8(d) had grown slightly thicker and the macrovoids formation was more uniform compared to untreated PVDF membrane surface as seen in Fig. 8(a). However, PVDF-g-PAAc membrane surface was densely modified with PAAc as observed in Fig. 8(g).

Likewise, in the appearance on the bottom surface, the membrane porosity after argon plasma treatment shown in Fig. 8(e) maintained the network structure of the untreated PVDF membrane surface represented by Fig. 8(b). On the other hand, PVDF-g-PAAc membrane surface shown in Fig. 8(h) was also grafted with PAAc gentler than the upper surface of PVDF-g-PAAc membrane as seen in Fig. 8(g). Therefore, for sustaining the high porosity of the upper surface, it would be preferable to treat with the intensity of plasma equivalent to be present against the bottom surface, but in that case, conjugation level of BSA on the upper surface might be decreased.

The cross sectional view of PVDF-g-PAAc membrane indicated in Fig. 8(i) showed that the PAAc was grafted onto the upper and pore surfaces within the bulk of the membrane. To investigate the degree of distribution structured by graft polymerization of AAc, we noted the cross sectional image of PVDF-g-PAAc membrane at a magnification of 750× as shown in Fig. 8(j). As the result of that, it was observed that each part described red and green arrows in the upper and bottom layer membrane of Fig. 8(j) respectively was uniformly grafted with PAAc, and then these individual depths were approximately 37 μm and 13 μm. Thus, as for PVDF-g-PAAc membrane, the graft yield in the upper of the membrane was expected to be approximately three times higher than in the bottom of that.

AFM operating in dynamic force mode was performed to study the surface topography of untreated PVDF, plasma-treated PVDF and PVDF-g-PAAc membrane. Table 4 reveals the surface roughness (*Ra*) of these membrane surfaces. The *Ra* was estimated from the AFM images on 5 μm × 5 μm lateral area.

Fig. 9 presents typical AFM images. From the results of Table 4, the *Ra* of argon plasma-treated PVDF membrane surface (46.6 nm; Fig. 9(b)) was a little decreased against that of untreated PVDF membrane surface (49.8 nm; Fig. 9(a)). The findings implied that the plasma condition for introducing functional groups was mild treatment against the membrane surface. On the other hand, we observed that there was shape like a high-density bumpy surface as shown in the AFM image on 500 nm × 500 nm lateral area (Fig. 9(e,

Table 4
Surface roughness of untreated PVDF membrane, PVDF membrane treated with argon plasma (treatment: ±4.0 kVp-p, 180 s) and PVDF-g-PAAc membrane (treatment: 20%(v/v) AAc, 70 °C, 30 min). The *Ra* was estimated from the AFM images on 5 μm × 5 μm lateral area.

Membranes	Calculated average roughness (*Ra*) (nm)
Untreated PVDF	49.8
Argon plasma-treated PVDF	46.6
PVDF-g-PAAc	5.9

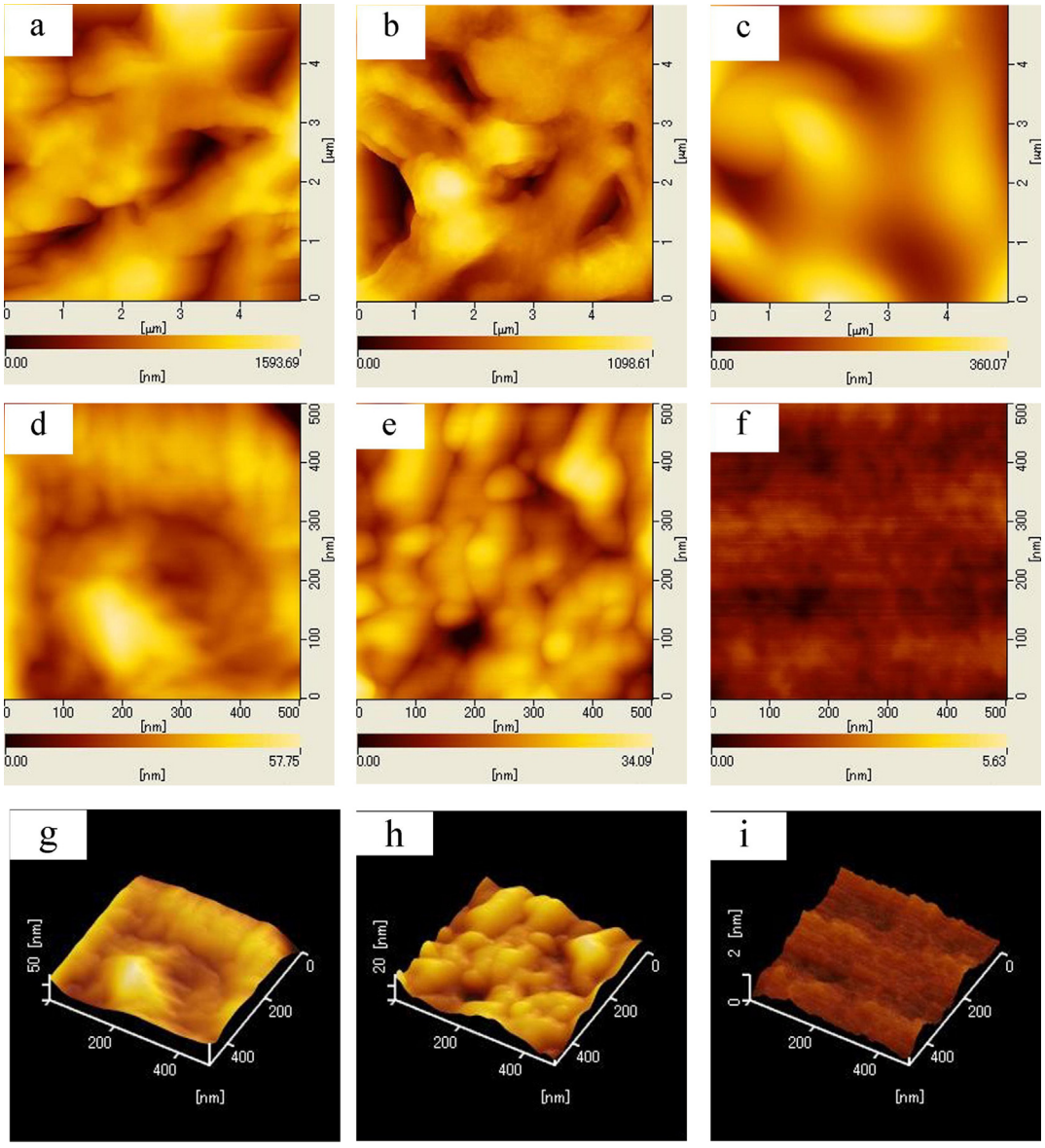

Fig. 9. Surface AFM images of untreated PVDF membrane (a, d, g), PVDF membrane treated with argon plasma (b, e, h; treatment: ±4.0 kVp-p, 180 s) and PVDF-g-PAAc membrane (c, f, i; treatment: 20%(v/v) AAc, 70 °C, 30 min). a, b, c: 5 μm × 5 μm lateral area; d, e, f, g, h, i: 0.5 μm × 0.5 μm lateral area.

h)). These topological changes could result from chemical reactions and sputter processes of the plasma species with the surface. The observed features were also presumed to be a consequence of melting or recrystallization processes [42]. Hence, we are convinced that the plasma treatment is capable of modifying chemical and topological changes on the membrane surface simultaneously. Furthermore, the *R*a of PVDF-g-PAAc membrane (5.9 nm; Fig. 9(c)) was smooth and uniform structural features compared to plasma-treated PVDF membrane surface (46.6 nm; Fig. 9(b)).

As it has been also observed by R. Morent et al., the surface morphology of the plasma deposited films (deposition time = 90 s) for the different discharge regions clearly showed that the surfaces of the plasma deposited polyacrylic acid membranes are quite smooth and that no significant differences in surface morphology can be found between the different discharge regions [48].

Taken together, we conclude that the plasma treatment is an excellent method to activate surface polymer of PVDF membrane, and plays an important role as pretreatment in fabricating chemically and physically uniform polymerized AAc membrane.

4. Conclusions

In this work, we have described a synthetic way to graft acrylic acid polymer on PVDF membrane surface using the cold atmospheric pressure plasma torch (CAPPLAT). The initiator of graft polymerization is mainly hydroperoxide, which decomposed into free radicals generated by argon plasma-induced activation, and we proposed the activation mechanism. The porosity of the membrane scaffold was preserved after the atmospheric pressure low temperature plasma treatment. Bovine serum albumin (BSA) was successfully conjugated on the polymer-modified PVDF membranes. The presence of BSA on the membranes was studied using high resolution XPS. The atmospheric pressure low temperature plasma is an easy, economic and effective method to covalently attach

hydrophilic polymers on PVDF membranes in order to produce PVDF-based devices for biotechnological application.

References

[1] Dargaville Tim R, George Graeme A, Hill David JT, Whittaker Andrew K. High energy radiation grafting of fluoropolymers. Prog Polym Sci 2003;9:1355.
[2] Cleland MR, Parks LA, Cheng S. Applications for radiation processing of materials. Nucl Instr Meth Phys Res B 2003;208:66.
[3] Johns Ken, Stead Gordon. Fluoroproducts – the extremophiles. J Fluor Chem 2000;104:5.
[4] Shi Tongna, Shao Meiling, Zhang Hongrui, Yang Qing, Shen Xinyuan. Surface modification of porous poly (tetrafluoroethylene) film via cold plasma treatment. Appl Surf Sci 2011;258:1474.
[5] Njatawidjaja Ellyana, Kodama Makoto, Matsuzaki Kenji, Yasuda Keishu, Matsuda Takehisa, Kogoma Masuhiro. Hydrophilic modification of expanded polytetrafluoroethylene (ePTFE) by atmospheric pressure glow discharge (APG) treatment. Surf Coatings Technol 2006;201:699.
[6] Young Tai-Horng, Chang Hsu-Hsien, Lin Dar-Jong, Cheng Liao-Ping. Surface modification of microporous PVDF membranes for neuron culture. J Membr Sci 2010;350:32.
[7] Hara Yasuhiro, Ooka Kento, Zettsu Nobuyuki, Yamamura Kazuya. Relationship between peroxide radical species on plasma-treated PFA surface and adhesion strength of PFA/electroless copper-plating film. Curr Appl Phys 2012;12:538.
[8] Okubo Masaaki, Tahara Mitsuru, Saeki Noboru, Yamamoto Toshiaki. Surface modification of fluorocarbon polymer films for improved adhesion using atmospheric-pressure nonthermal plasma graft-polymerization. Thin Solid Films 2008;516:6592.
[9] Rosenberg Y, Siegmann A, Narkis M, Shkolnik S. Low dose γ-irradiation of some fluoropolymers: effect of polymer chemical structure. J Appl Polym Sci 1992;45:783.
[10] Leivo E, Wilenius T, Kinos T, Vuoristo P, Mäntylä T. Properties of thermally sprayed fluoropolymer PVDF, ECTFE, PFA and FEP coatings. Prog Org Coatings 2004;49:69.
[11] Liu Fu, Awanis Hashim N, Liu Yutie, Moghareh Abed MR, Li K. Progress in the production and modification of PVDF membranes. J Membr Sci 2011;375:1.
[12] Kuriyel Ralf, Zydney Andrew L. Sterile filtration and virus filtration. Methods Biotechnol 2000;9:185.
[13] Ritchie Stephen MC, Kissick Kyle E, Bachas Leonidas G, Sikdar Subhas K, Parikh Chetan, Bhattacharyya Dibakar. Polycysteine and other polyamino acid functionalized microfiltration membranes for heavy metal capture. Environ Sci Technol 2001;35:3252.
[14] Ritchie SMC, Bachas LG, Olin T, Sikdar SK, Bhattacharyya D. Surface modification of silica- and cellulose-based microfiltration membranes with functional polyamino acids for heavy metal sorption. Langmuir 1999;15:6346.
[15] Singh Nripen, Husson Scott M, Zdyrko Bogdan, Luzinov Igor. Surface modification of microporous PVDF membranes by ATRP. J Membr Sci 2005;262:81.
[16] Nasef Mohamed Mahmoud, Güven Olgun. Radiation-grafted copolymers for separation and purification purposes: status, challenges and future directions. Prog Polym Sci 2012;37:1597.
[17] Ulbricht Mathias. Advanced functional polymer membranes. Polymer 2006;47:22.
[18] Han Man Jae, Baroña Garry Nathaniel B, Jung Bumsuk. Effect of surface charge on hydrophilically modified poly (vinylidene fluoride) membrane for microfiltration. Desalination 2011;270:76.
[19] Kalbfuss Bernd, Wolff Michael, Geisler Liane, Tappe Alexander, Wickramasinghe Ranil, Thom Volkmar, et al. Direct capture of influenza A virus from cell culture supernatant with sartobind anion-exchange membrane adsorbers. J Membr Sci 2007;299:251.
[20] Kosior Anna, Antošová Monika, Faber Rene, Villain Louis, Polakovič Milan. Single-component adsorption of proteins on a cellulose membrane with the phenyl ligand for hydrophobic interaction chromatography. J Membr Sci 2013;442:216.
[21] Sun Haixiang, Zhang Lin, Chai Hong, Yu Ji, Qian Hua, Chen Huanlin. A study of human γ-globulin adsorption capacity of PVDF hollow fiber affinity membranes containing different amino acid ligands. Sep Purif Technol 2006;48:215.
[22] Zhang Mo, Zhang Lin, Cheng Li-Hua, Xu Kun, Xu Qiu-Ping, Chen Huan-Lin, et al. Extracorporeal endotoxin removal by novel l-serine grafted PVDF membrane modules. J Membr Sci 2012;405–406:104.
[23] Teeters MA, Conrardy SE, Thomas BL, Root TW, Lightfoot EN. Adsorptive membrane chromatography for purification of plasmid DNA. J Chromatogr 2003;989:165.
[24] Woo Maybelle, Khan Navid Z, Royce Jonathan, Mehta Ushma, Gagnon Brian, Ramaswamy Senthil, et al. A novel primary amine-based anion exchange membrane adsorber. J Chromatogr 2011;1218:5386.
[25] Wang Lu, Ghosh Raja. Fractionation of monoclonal antibody aggregates using membrane chromatography. J Membr Sci 2008;318:311.
[26] Park YW, Inagaki N. Surface modification of poly (vinylidene fluoride) film by remote Ar, H_2, and O_2 plasmas. Polymer 2003;44:1569.
[27] Chu PK, Chen JY, Wang LP, Huang N. Plasma-surface modification of biomaterials. Mater Sci Eng 2002;36:143.
[28] Pascu M, Nicolas D, Poncin-Epaillard F, Vasile C. Surface modification of PVDF by plasma treatment for electroless metallization. J Optoelectron Adv Mater 2006;8:1062.
[29] Duca Mariana D, Plosceanu Carmina L, Pop Tatiana. Surface modifications of polyvinylidene fluoride (PVDF) under rf Ar plasma. Polym Degrad Stab 1998;61:65.
[30] Muller M, Oehr C. Plasma aminofunctionalisation of PVDF microfiltration membranes. Surf Coatings Technol 1999;116-119:802.
[31] Oehr Christian. Plasma surface modification of polymers for biomedical use. Nucl Instr Meth Phys Res B 2003;208:40.
[32] Mazzei Ruben, Smolko Eduardo, Tadey Daniel, Gizzi Laura. Radiation grafting of NIPAAm on PVDF nuclear track Membranes. Nucl Instr Meth Phys Res B 2000;170:419.
[33] Forsythe JS, Hill DJT. The radiation chemistry of fluoropolymers. Prog Polym Sci 2000;25:101.
[34] Berthelot Thomas, Le Xuan Tuan, Jégou Pascale, Viel Pascal, Boizot Bruno, Baudin Cécile, et al. Photoactivated surface grafting from PVDF surfaces. Appl Surf Sci 2011;257:9473.
[35] Lubarsky GV, Davidson MR, Bradley RH. Characterisation of polystyrene microspheres surface-modified using a novel UV-ozone/fluidised-bed reactor. Appl Surf Sci 2004;227:268.
[36] Deng Jianping, Wang Lifu, Liu Lianying, Yang Wantai. Developments and new applications of UV-induced surface graft polymerizations. Prog Polym Sci 2009;34:156.
[37] Zhang Minggang, Nguyen Quang Trong, Ping Zhenghua. Hydrophilic modification of poly (vinylidene fluoride) microporous membrane. J Membr Sci 2009;327:78.
[38] Chen Yiwang, Deng Qilan, Xiao Jichun, Nie Huarong, Wu Lichuan, Zhou Weihua, et al. Controlled grafting from poly (vinylidene fluoride) microfiltration membranes via reverse atom transfer radical polymerization and antifouling properties. Polymer 2007;48:7604.
[39] He Dongming, Susanto Heru, Ulbricht Mathias. Photo-irradiation for preparation, modification and stimulation of polymeric membranes. Prog Polym Sci 2009;34:62165.
[40] Yamago Shigeru, Nakamura Yasuyuki. Recent progress in the use of photoirradiation in living radical polymerization. Polymer 2013;54:981.
[41] Tendero Claire, Tixier Christelle, Tristant Pascal, Desmaison Jean, Leprince Philippe. Atmospheric pressure plasmas: a review. Spectrochim Acta Part B 2006;61:2.
[42] Noeske Michael, Degenhardt Jost, Strudthoff Silke, Lommatzsch Uwe. Plasma jet treatment of five polymers at atmospheric pressure: surface modifications and the relevance for adhesion. Int J Adhesion Adhesives 2004;24:171.
[43] Merche Delphine, Vandencasteele Nicolas, Reniers François. Atmospheric plasmas for thin film deposition: a critical review. Thin Solid Films 2012;520:4219.
[44] Chen Mingsheng, Zhang Ying, Yao Xiaomei, Li Hao, Yu Qingsong, Wang Yong. Effect of a non-thermal, atmospheric-pressure, plasma brush on conversion of model self-etch adhesive formulations compared to conventional photopolymerization. Dent Mater 2012;28:1232.
[45] Gu Minghao, Kilduff James E, Belfort Georges. High throughput atmospheric pressure plasma-induced graft polymerization for identifying protein-resistant surfaces. Biomaterials 2012;33:1261.
[46] Kato Koichi, Uchida Emiko, Kang En-Tang, Uyama Yoshikimi, Ikada Yoshito. Polymer surface with graft chains. Prog Polym Sci 2003;28:209.
[47] Goddard JM, Hotchkiss JH. Polymer surface modification for the attachment of bioactive compounds. Prog Polym Sci 2007;32:698.
[48] Morent R, De Geyter N, Van Vlierberghe S, Beaurain A, Dubruel P, Payen E. Influence of operating parameters on plasma polymerization of acrylic acid in a mesh-to-plate dielectric barrier discharge. Prog Org Coatings 2011;70:336.
[49] Kuwabara Atsushi, Kuroda Shin-ichi, Kubota Hitoshi. Development of atmospheric pressure plasma low temperature surface discharge plasma torch and application to polypropylene surface treatment. Plasma Chem Plasma Process 2008;28:263.
[50] Mizote Norihito, Kuroda Shin-ichi. Friction characteristics of amorphous carbon films on rubber deposited by cold atmospheric pressure plasma. Tribol Online 2012;7:234.
[51] Hidzir Norsyahidah Mohd, Hill David JT, Martin Darren, Grøndahl Lisbeth. Radiation-induced grafting of acrylic acid onto expanded poly(tetrafluoroethylene) membranes. Polymer 2012;53:6063.
[52] Liu Fu, Du Chun-Hui, Zhu Bao-Ku, Xu You-Yi. Surface immobilization of polymer brushes onto porous poly (vinylidene fluoride) membrane by electron beam to improve the hydrophilicity and fouling resistance. Polymer 2007;48:2910.
[53] W.L. Wiese, M.W. Smith and B.M. Miles. Atomic transition probabilities, NSRDS-NBS 22, Washington, DC, 1969.
[54] Matienzo LJ, Zimmerman JA, Egitto FD. Surface modification of fluoropolymers with vacuum ultraviolet irradiation. J Vac Sci Technol A 1994;12:2662.